Fabrication of organic solar array for applications in microelectromechanical systems

Jason Lewis, Jian Zhang, and Xiaomei Jiang[a)]
Department of Physics, University of South Florida, Tampa, Florida 33620, USA

(Received 11 August 2008; accepted 11 September 2008;
published online 6 November 2008)

We have developed an innovative way to fabricate organic solar arrays for application in dc power supplies for electrostatic microelectromechanical systems devices. A solar array with 20 miniature cells interconnected in series was fabricated and characterized. Photolithography was used to isolate the individual cells and output contacts of the array, whereas the thermal-vacuum deposition is employed to make the series connections of the array. With 1 mm^2 for single cell and a total device area of 2.2 cm^2, the organic solar array based on bulk heterojunction structure of π-conjugated polymers and C_{60} derivative [6,6]-phenyl C_{61} butyric acid methyl ester produced an open-circuit voltage of 7.8 V and a short-circuit current of 55 μA under simulated air mass (AM) 1.5 illumination with an intensity of 132 mW/cm^2. The procedure described here has the full potential for use in future fabrication of microarray with the size as small as 0.01 mm^2. © *2009 American Institute of Physics.* [DOI: 10.1063/1.2998825]

I. INTRODUCTION

Microelectromechanical systems (MEMS) usually have their own requirements for power supplies. It is desirable to have appropriate on-chip power source with the MEMS device, particularly in cases of autonomous operations such as wireless communication, sensor network, and microrobotic systems. Previous solutions for such power supplies include magnetic field induced current and voltage supplies,[1] electrothermal microactuators based on dielectric loss heating,[2] rechargable lithium microbatteries,[3] integrated thermopile structures,[4] vibration-electric energy conversion,[5] and miniature fuel cells.[6]

Solar cell can also be a good option for such power sources since it is self-contained and can be easily integrated with existing circuits of MEMS. Moreover, solar cell has the potential of achieving the maximum size to power density ratio compared with other miniature power sources.[7] There have been previous studies about on-chip solar cell arrays for applications in MEMS devices,[7–11] and the majority of these works have been related to the silicon photovoltaic cells.

Organic solar cells (OSC) based on π-conjugated polymers [e.g., poly-3-hexylthiophene (P3HT)] and fullerene derivatives [e.g., (6,6)-phenyl C_{61} butyric acid methyl ester (PCBM)] have attracted attention over the past decades because they may provide a cost-effective route to wide use of solar energy for electrical power generation.[12–16] These organic semiconductors have the advantage of being chemically flexible for material modifications, as well as mechanically flexible for the prospective of low-cost, large scale processing such as solution-cast on flexible substrates. The world's next generation of microelectronics may be dominated by "plastic electronics'" and organic solar cells are expected to play an important role in these future technologies.[17]

The photovoltaic process in OSC devices consists of four successive processes: light absorption, exciton dissociation, charge transport, and charge collection: (i) Absorption of a photon

[a)]Author to whom correspondence should be addressed. Electronic mail: xjiang@cas.usf.edu.

creates an exciton (bounded electron-hole pair); (ii) the exciton diffusion to a region (for instance, the interface of two different components), where exciton dissociation (or charge separation) occurs; (iii) finally, free charges move separately toward the anode (holes) and cathode (electrons), where (iv) they are collected. Several parameters determine the performance of a solar cell, namely, the open-circuit voltage (V_{oc}), short-circuit current (I_{sc}), and the so-called fill factor (FF). FF is calculated by

$$\mathrm{FF} = \frac{I_{mp} V_{mp}}{I_{sc} V_{oc}}, \tag{1}$$

where I_{mp} and V_{mp} are the current and voltage operating points for maximum power, respectively. The overall power conversion efficiency η is defined as

$$\eta = \frac{I_{mp} V_{mp}}{P_{in}} = \frac{\mathrm{FF} \cdot I_{sc} V_{oc}}{P_{in}}. \tag{2}$$

Although the current power conversion efficiency (about 6%) of OSC is still not high enough to make it a practical solution for large scale commercial applications as general electric power sources, it is promising to use OSC as a high-voltage power supply. The open-circuit voltage of single junction OSC (V_{oc}=0.6–0.7 eV) is close to that of the single crystal Si or thin film polycrystalline Si.[8] For many electrostatic MEMS, it is more critical to have high-voltage output (from tens to hundreds of volts) rather than high current or energy efficiency, with an operatable current range usually falling between nanoamperes to microamperes. According to the design criteria of such on-chip solar cells,[8] OSC based on π-conjugated polymers and fullerene derivatives is an excellent choice. First of all, isolation of the solar cell array from the MEMS substrate is easy to achieve, since OSC can be fabricated on any substrate including plastic. This also makes the integration with microsensors and microactuators relatively effortless. Second, these polymers are efficient light absorbers (with a typical absorption coefficient several orders higher than that of the conventional semiconductors such as Si), meaning the active layer can be as thin as 100 nm, which makes it simple for series interconnection to produce high voltage. Third, V_{oc} of a single cell of these OSCs can be easily tuned as high as 0.87 V by chemical tailoring of both constituents.[18] Fourth, the photoactive layer can be made through any solution processable fabrication methods (i.e., spin-coating, spraying, and inkjet printing) without the need of photolithography, which is mandatory with silicon-related fabrication process. These OSC can be manufactured on plastic substrates, making these cells lightweight, flexible, and very cost-effective. The usual drawbacks of OSC (e.g., lower short-circuit current and power conversion efficiency) are not the major issues for using them as on-chip dc power sources, making OSC a perfect solution for MEMS inertia transducers, such as resonator, accelerometer, gyroscope, and pressure sensors.[19]

To the best of our knowledge, there has been no report of organic solar arrays based on P3HT and PCBM as MEMS power sources. Although there have been previous studies on large area organic solar modules.[20–23] A small (2.2 cm^2) photovoltaic minimodule having 20 cells in series was reported in this article. The anode is made by patterning indium tin oxide (ITO) on glass by photolithography, the cathode is made by thermal evaporation through a metal shadow mask, which simultaneously accomplishes the series connection of all cells. The active layer material used in our process is a blend of P3HT and PCBM, which forms a bulk heterojunction structure. In this report, a detailed array fabrication process and the characterization of both single cell and interconnected solar array are present. In the end, a brief discussion will be given about the factors that could affect the output voltage and overall power efficiency, as well as several tentative solutions for short-circuit problems within the array. Our research has focused on the design of a process to ensure full isolation of series connected cells, and this process has the full potential for use in future fabrication of a microarray with a size as small as 0.01 mm^2.

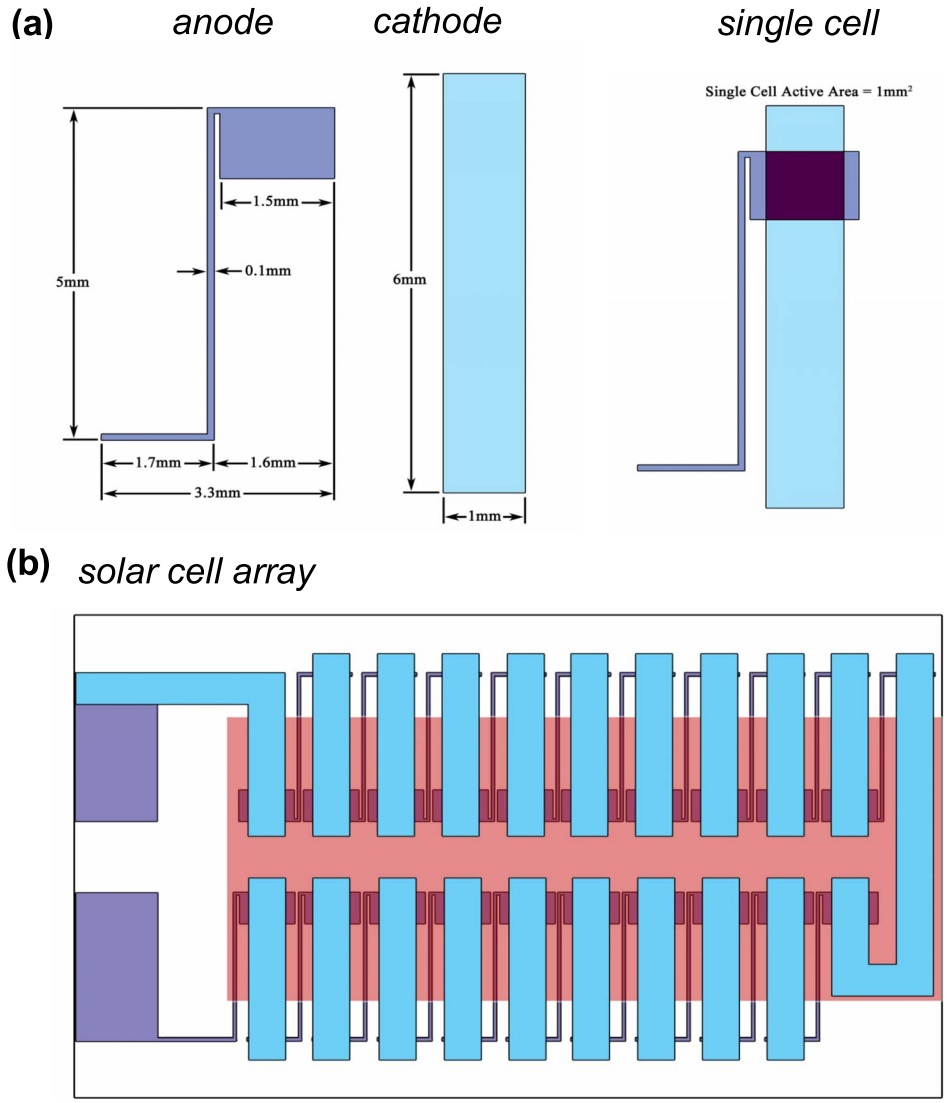

FIG. 1. (a) Enlarged drawing of the anode, cathode, and sandwich structure of single cell with area of 1 mm^2. (b) Illustration of the interdigitated organic solar cell array consisted of 20 single cells. The bottom (light purple) layer is photolithography-defined ITO anode, the middle (red) layer is spin-coated P3HT:PCBM, and the top (light blue) layer is thermal deposited cathode by shallow mask technique.

II. FABRICATION PROCESS

The first step was the design of the solar array. The ability to align the substrate with the shadow mask by eye in the inert environment as well as other process parameters were considered before a final geometric design was made for the array. Figure 1 shows such an array consisting of 20 single cells. The top panel of Fig. 1 presents details of each cell. The whole fabrication process consists of four steps.

A. Patterning of the anode

ITO coated glass substrates (>85% transmittance, 5–15 $\Omega/\square$) were purchased from Delta Technology Inc. and cut into 1 in.$\times$1 in. pieces. The patterning of ITO is done via standard photolithography using a custom made photomask, as shown in Fig. 1 (light purple). The photomask was made by printing the desired pattern on one plastic transparency and taped onto a piece

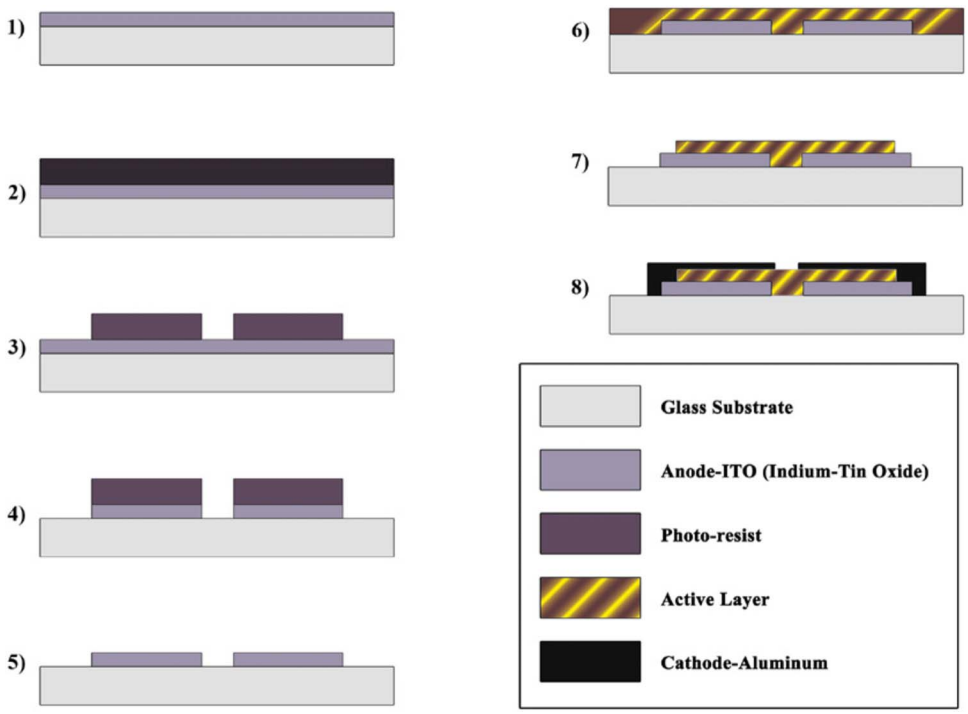

FIG. 2. The fabrication process of miniature solar cell array. Start from (1) a clean ITO on glass substrate, followed by (2) spin-coating photoresistance, (3) development of desired pattern by photolithography, (4) etching off the unwanted ITO, (5) washing off the photoresistance, (6) spin-coating active layer (P3HT:PCBM), (7) clean off excessive material, (8) deposit cathode via shadow mask.

of 5 in.$\times$5 in. glass. Positive photoresist (Shipley 1813) is spun-coat onto the ITO side of the substrate at a rate of 4500 rpm for 45 s, creating a layer with thickness of about 1.5 μm. The substrate is then soft baked on a 90 °C hotplate for 90 s, followed by a 3 s exposure to UV light through the photomask, and the substrate is then developed in Shipley MF319 for about 1 min, followed by a hard bake at 150 °C for 10 min. Etching of the ITO was done in a mixed solution of HCl and HNO_3. The patterned ITO substrate then undergoes sonification cleaning in trichloroethylene, acetone, and isopropanol at 50 °C for 20 min each, followed by drying with N_2. The glass substrate now has the desired pattern of ITO, which acts as the anode part of the solar array.

B. Creation of the shadow mask

A 1 in.$\times$1 in. piece of stainless steel was patterned following a similar photolithography procedure described above. Etching of the photoresist coated stainless steel was done using a diluted ferric chloride ($FeCl_3$) solution [25% in deionized (DI) water] for 2 h. The patterned shadow mask (Fig. 1, light blue) was rinsed by DI water and sonification in acetone and isopropanol at 50 °C for 20 min.

C. Formation of the photoactive layer

The original aqueous poly(3,4ethylenedioxythiophene):poly(styrenesulfonate) (PEDOT:PSS) (Baytron 500) obtained from H. C. Starck was diluted and filtered three times, then filtered out through a 0.45 μm filter. The solution is then spun coat on top of the patterned ITO at a rate of 5000 rpm for 90 s after which the substrate is then heated up to 120 °C for 100 min. P3HT and PCBM were purchased from American Dye Source Inc. The active layer solution is made by mixing P3HT and PCBM with a weight ratio of 1:1 in chloroform, then spun-coat on top of the PEDOT:PSS coated substrate at a rate of 700–800 rpm for 90 s. This provides a thickness of

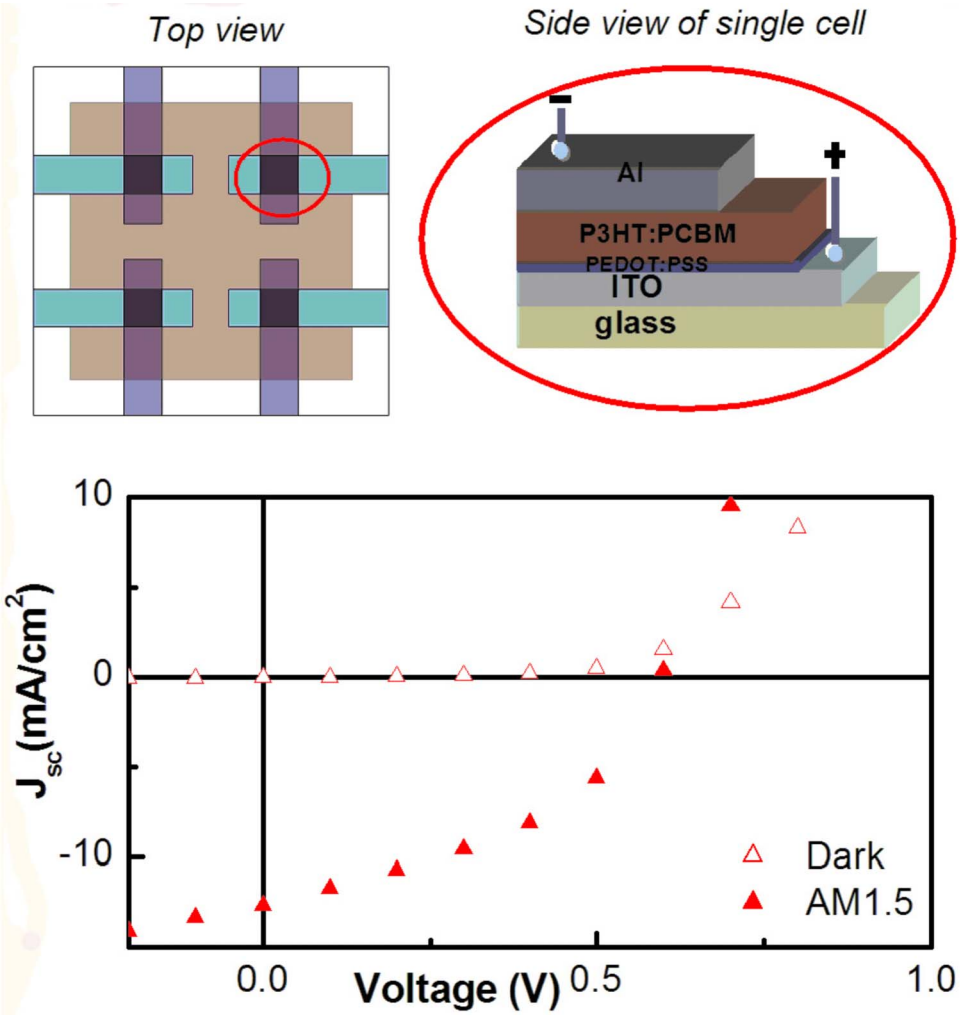

FIG. 3. Upper panel: schematic of a single organic solar cell with bulk heterojunction structure. Lower panel: current-voltage characteristics of single cell made with P3HT:PCBM mixed with weight ratio of 1:1 under simulated AM1.5G, radiation at 132.6 mW/cm^2. The active layer was spun-coat on patterned ITO substrate at 800 rpm, with a final thickness of about 200 nm. Post-device thermal annealing at 120 °C for 5 min was done before the *I-V* measurements.

200 nm. The excess film is then wiped off in order to allow the aluminum to make the series connections required for the device (Fig. 1). The sample is then allowed to dry for a minimum of 3 h in vacuum before thermal evaporation of the cathode.

D. Deposition of the cathode

In order for the device to function as a series array, the patterned shadow mask must be precisely aligned to the ITO substrate (see Fig. 1). With the alignment done the substrate is then fixed onto the chuck and loaded into the deposition chamber. Aluminum was chosen for the cathode due to its desirable work function (for collection of electrons) and cost-effectiveness. Deposition of aluminum was done under high vacuum ($>10^{-7}$ torr), with a final thickness of 100 nm. Device fabrication is completed with a final annealing on a hotplate at 110 °C for 5 min in the glove box, prior to the *I-V* measurements.

Figure 2 illustrates the fabrication process for the organic solar array. The active layer is spun-coat from a chloroform solution of P3HT:PCBM blend with a weight ratio of 1:1.

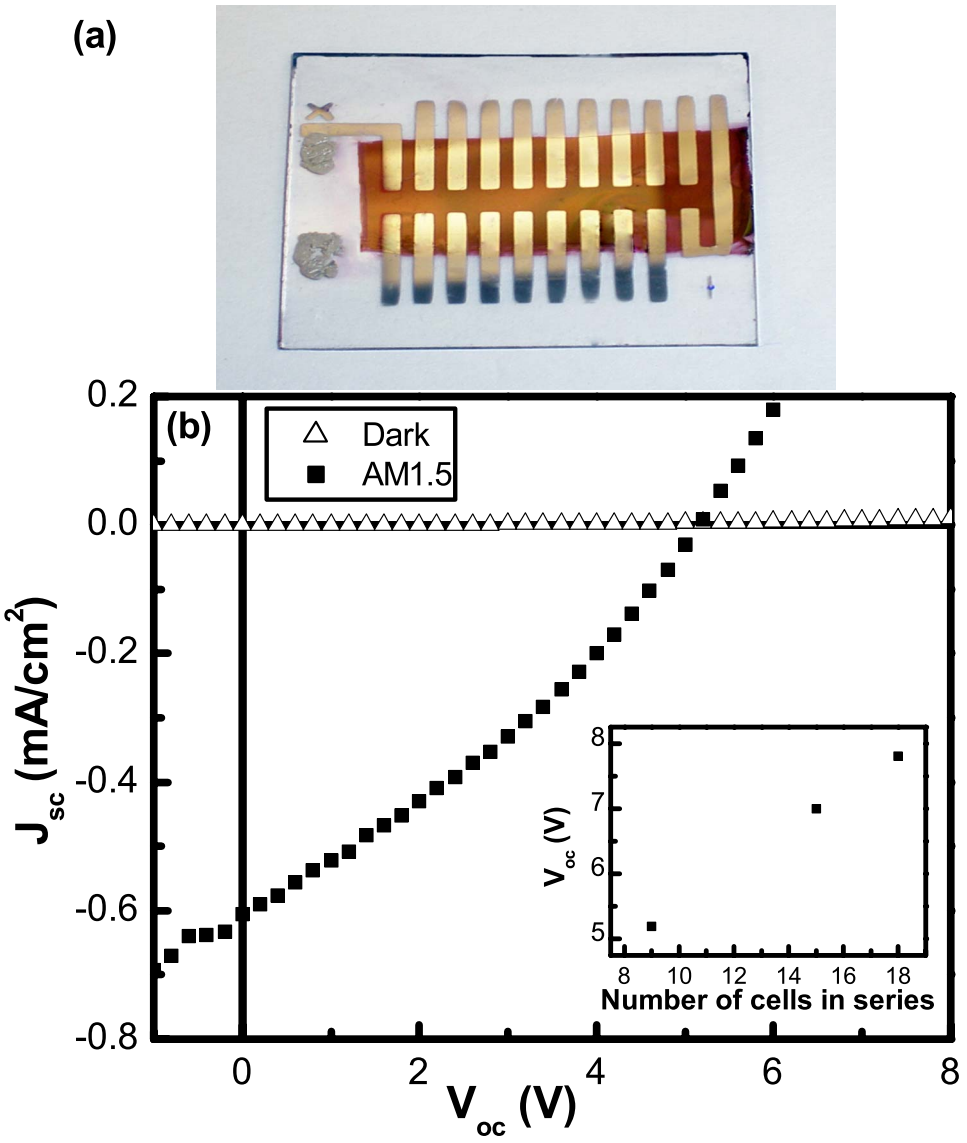

FIG. 4. (a) A digital picture of the organic solar array with 20 miniature cells in series, (b) current-voltage curve of an organic solar array with nine functioning cells measured at simulated AM1.5G with radiation of 132.6 mW/cm^2. The fabrication parameters are the same as single cell (in Fig. 3). The inset shows array V_{oc} as a function of number of cells in series. An output voltage of 7.8 V was achieved with 18 cells in series.

III. EXPERIMENTAL RESULTS

In order to examine the solar array fabrication procedure described above and find the operational parameters for various processes, we fabricated test OSC in a simpler geometry consisting of four single cells, each has an active area of 4 mm^2 (Fig. 3 upper left panel). The upper right panel of Fig. 3 shows the side view of each cell in bulk heterojunction structure. Preliminary optimization was performed in terms of spin rate and thermal annealing conditions. The best performed single cell was fabricated with an active layer thickness of 200 nm followed by a post-device thermal annealing at 120 °C for 5 min.

The current-voltage (I-V) characterization of the solar cells was performed on a solar simulator consisting of a xenon arc lamp (Oriel 66485) and an air mass (AM) 1.5 global filter (Oriel 81094) with irradiation of 132.6 mW/cm^2. No spectral mismatch with the standard solar spectrum

TABLE I. Summary of device parameters for three organic solar cell arrays containing different numbers of cells in series. The current voltage characteristics in dark and under simulated solar AM1.5 with an intensity of 132.6 mW/cm^2 are present. Each cell has an active area of 1 mm^2. The power conversion efficiency (η) was calculated using Eq. (2) in text.

Array name	Active layer thickness (nm)	Number of cells in series	V_{oc} (V)	I_{sc} (mA)	J_{sc} (mA/cm^2)	FF	η (%)
Array 1	203	9	5.2	0.0545	0.605	0.32	0.76
Array 2	202	15	7.0	0.0245	0.163	0.17	0.15
Array 3	232	18	7.8	0.0135	0.075	0.13	0.06

AM 1.5 (with an intensity of 132 mW/cm^2) was corrected in the I-V characterization. The best of such single devices has a short-circuit current density J_{sc}=12.7 mA/cm^2, open-circuit voltage V_{oc}=0.60 V, FF=0.43, and a power conversion efficiency of 2.45% (Fig. 3 lower panel). While this modest efficiency certainly has room to be improved by nanomorphology manipulations,[15,16] the main purpose herein is to find the right parameters for each fabrication process.

Using these appropriate parameters, organic solar cell array based on the same photoactive material (P3HT and PCBM blend) used above was fabricated according to the fabrication procedure described in Sec. II. The interconnected series consists of 20 cells each with active area of 1 mm^2 on a 1 in.^{2} ITO substrate. A picture of such an array is shown in Fig. 4(a). Figure 4(b) shows the I-V curve of the best performed array (array 1 in Table I). Though extra caution and efforts have been made to avoid short circuits among individual cells, the alignment of shadow mask with the ITO anodes inside the glove box turned out to be very challenging, especially when the active layer is thin (<200 nm). Not-so-perfect alignment resulted in "shadow effect," which smeared out the contact to neighboring cells, causing unintentional lateral connection.

In this preliminary work, we also tried to increase the active layer thickness to see how it would help with short circuits of individual cells. Table I gives a summary of three solar arrays with different active layer thicknesses. It can be seen that, with thicker film, a smaller number of cells was short circuited. The inset of Fig. 4(b) plots the array V_{oc} versus the number of cells in series, and a linear relation is shown; for a total of 18 minicells, the measured V_{oc} is 7.8 V.

Although the overall device performance is less impressive, and the poor FF might be due to increased lateral collection, causing the increase of series resistance (R_s) of the solar array.[11] The more important point is the capability to obtain larger V_{oc} in terms of the application for dc power supply. Our prefactory results demonstrate the potential to easily tune the output voltage by the number of cells in series. Further improvement of the array performance is ongoing to determine the optimization of active layer thickness and nanomorphology, as well as to reduce R_s of the array device by means of thermal annealing and modifying the contact properties between active layer and the electrodes.

IV. CONCLUSION

In conclusion, a miniature organic solar array was designed, fabricated, and characterized for application in MEMS device power supplies. The photoactive layer was formed by spin coating a thin film of π-conjugated polymer P3HT and fullerene derivative PCBM blend mixed in chloroform. The electrodes were patterned by photolithography and thermal evaporation through a patterned shadow mask. An output voltage of 7.8 V and short-circuit current as large as 55 μA under simulated solar AM1.5 illumination were achieved with the small array device (2.2 cm^2).

ACKNOWLEDGMENTS

The authors are grateful for the financial support from USF Grant No. GFMMD03, ACS Petroleum Research Fund (PRF 47107-G10) and the U.S. Department of Army USAMRMC Grant No. W81XWH-07-1-0708. We would also like to acknowledge Robert Tufts and Richard Everly for their help with USF NNRC facilities and training.

[1] H. Matsuki, M. Yamaguchi, T. Watanabe, and K. Murakami, J. Appl. Phys. **64**, 5859 (1988).
[2] B. Rashidian and M. G. Allen, in *Proceedings of the 6th IEEE Workshop on Micro Electro Mechanical Systems, Fort Lauderdale, FL, February 1993* (IEEE, Piscataway, NJ, 1993), p. 24.
[3] J. B. Bates, G. R. Gruzalski, and C. F. Luck, in *Proceedings of the 6th IEEE Workshop on Micro Electro Mechanical Systems, Fort Lauderdale, FL, February 1993* (IEEE, Piscataway, NJ, 1993), p. 82.
[4] Z. Olgun, O. Akar, H. Kulah, and T. Akin, in *Proceedings of the Transducers 97, International Conference on Solid-State Sensors and Actuators* (IEEE, New York, 1997), p. 1263.
[5] S. Meninger, J. O. Mur-Miranda, R. Amirtharajah, A. Chandrakasan, and J. Lang, in *Proceedings of the 1999 International Symposium on Low Power Electronics and Design* (IEEE, New York, 1999), p. 48.
[6] A. Jansen, S. van Leeuwen, and A. Stevels, in *Proceedings of the 2000 IEEE International Symposium on Electronics and the Environment* (IEEE, Piscataway, NJ, 2000), p. 155.
[7] P. Ortega, S. Bermejo, and L. Castañer, IEEE Trans. Compon., Packag. Manuf. Technol., Part B **24**, 169 (2001).
[8] J. B. Lee, Z. Chen, M. G. Allen, A. Rohatgi, and R. Arya, J. Microelectromech. Syst. **4**, 102 (1995).
[9] S. Bermejo and L. Castañer, in *Proceedings of the 19th European Photovoltaic Solar Energy Conference and Exhibition*, Paris, France, 2CV.2.69, 2004, p. 135.
[10] M. A. Kroon, R. A. C. M. M. van Swaaij, and J. W. Metselaar, in *Proceedings of the 16th European Photovoltaic Solar Energy Conference* (James & James (Science Publishers) Ltd., London, 2000), p. 486.
[11] S. Bermejo, P. Ortega, and L. Castañer, Prog. Photovoltaics **13**, 617 (2005).
[12] G. Yu, J. Gao, J. C. Hummelen, F. Wudl, and A. J. Heeger, Science **270**, 1789 (1995).
[13] S. E. Shaheen, C. J. Brabec, N. S. Sariciftci, F. Padinger, T. Fromherz, and J. C. Hummelen, Appl. Phys. Lett. **78**, 841 (2001).
[14] M. M. Wienk, J. M. Kroon, W. J. H. Verhees, J. Knol, J. C. Hummelen, P. A. van Hal, and R. A. J. Janssen, Angew. Chem., Int. Ed. **42**, 3371 (2003).
[15] W. Ma, C. Yang, X. Gong, K. Lee, and A. J. Heeger, Adv. Funct. Mater. **15**, 1617 (2005).
[16] M. Reyes-Reyes, K. Kim, and D. L. Carroll, Appl. Phys. Lett. **87**, 083506 (2005).
[17] G. Dennler and N. S. Sariciftci, Proc. IEEE **93**, 1429 (2005).
[18] F. B. Kooistra, J. Knol, F. Kastenberg, L. M. Popescu, W. J. H. Verhees, J. M. Kroon, and J. C. Hummelen, Org. Lett. **9**, 551 (2007).
[19] N. V. Lavrik, M. J. Sepaniak, and P. G. Datskos, Rev. Sci. Instrum. **75**, 2229 (2004).
[20] S. Yoo, W. J. Potscavage, B. Domercq, J. Kim, J. Holt, and B. Kippelena, Appl. Phys. Lett. **89**, 233516 (2006).
[21] F. C. Krebs, H. Spanggard, T. Kjær, M. Biancardo, and J. Alstrup, Mater. Sci. Eng., B **138**, 106 (2007).
[22] C. Lungenschmied, G. Dennler, H. Neugebauer, S. N. Sariciftci, M. Glatthaar, T. Meyer, and A. Meyer, Sol. Energy Mater. Sol. Cells **91**, 379 (2007).
[23] M. Niggemann, B. Zimmermann, J. Haschke, M. Glatthaar, and A. Gombert, Thin Solid Films **516**, 7181 (2008).